INTERNATIONAL JOURNAL OF INTEGRATED ENGINEERING
ISSN: 2229-838X e-ISSN: 2600-7916

IJIE

Vol. 16 No. 8 (2024) 267-278
https://publisher.uthm.edu.my/ojs/index.php/ijie

Mathematical Modelling of Vehicle Rear End Design Using The Polynomial Response Surface Method (PRSM)

Kausalyah Venkatason[1]*, Walferd Cornell[1], Shasthri Sivaguru[2]

[1] *School of Mechanical Engineering, College of Engineering, Universiti Teknologi MARA, 40450 Shah Alam, Selangor, MALAYSIA*
[2] *School of Engineering & Physical Sciences, Heriot-Watt University Malaysia, Putrajaya, MALAYSIA*

*Corresponding Author: kausalyah@uitm.edu.my
DOI: https://doi.org/10.30880/ijie.2024.16.08.027

Article Info

Received: 3 July 2024
Accepted: 24 October 2024
Available online: 30 December 2024

Keywords

Sedan vehicle, coefficient of drag, mathematical modelling, CFD analysis, Polynomial Response Surface Method (PRSM)

Abstract

It is important to consider the aerodynamic efficiency of the car in design as it improves fuel consumption and provides a smoother ride for the occupant. Studies have shown that vehicle front end profile affects the aerodynamic efficiency of a car but however, to date rear-end vehicle parametric studies have not been done to ascertain the influence of these parameters on the vehicle's aerodynamic efficiency. This research presents the aerodynamic study of the sedan vehicle rear end by identification of the key vehicle rear-end parameters that influence the drag coefficient value of the vehicle model through the Polynomial Response Surface Modelling (PPRSM.). A total of 100 sedan vehicle models with 7 key rear end parameters generated through the Central Composite Design (CCD) sampling technique are designed using the CAD software, CATIA V5 R20. The front end of the vehicle profile is kept constant. Computational Fluid Dynamic Analysis (CFD) is then performed on these models to obtain the drag coefficient (Cd). Mathematical modelling is performed on the Cd data obtained using the PRSM method. The results from the PRSM model gave a value of R^2 is 0.926 with a relatively small error of RMSE at 0.006986 indicating a very good model fit. The rear end vehicle parameter that notably influenced the drag coefficient is the wind shield angle (X6) with the value from 21° to 41°. In conclusion, the rear end vehicle parameters do not seem to largely contribute to the aerodynamic stability of the model.

1. Introduction

In the ever-evolving landscape of automotive engineering, the pursuit of enhanced safety, efficiency, and performance remains paramount. Among the various aspects that demand meticulous attention, vehicle's parametric design holds a pivotal position [1]. When designing a new car, it is important to ensure that the design can reduce the aerodynamic drag, which can have a huge impact on the fuel consumption of the car and enhance the occupant's comfort [2]-[4]. Besides that, reducing the aerodynamic drag would also reduce the lift force of the vehicle [5], [6]. The vehicle's rear-end design has been traditionally optimised thus far by adding features that are able to reduce the drag coefficient values [7]-[9]. But till date no rear-end parametric design analysis has been done to identify key contributing parameters to vehicle drag coefficient. It is a domain where small adjustments can yield substantial improvements in vehicle safety, aerodynamics, and overall functionality. It has however been shown that adding pieces like a spoiler, wings, diffuser, and a vortex generator can have an impact on the vehicle's

drag coefficient since these features aid to reduce drag coefficient by creating turbulence in the air when it meets the part, which reduces drag [7], [10].

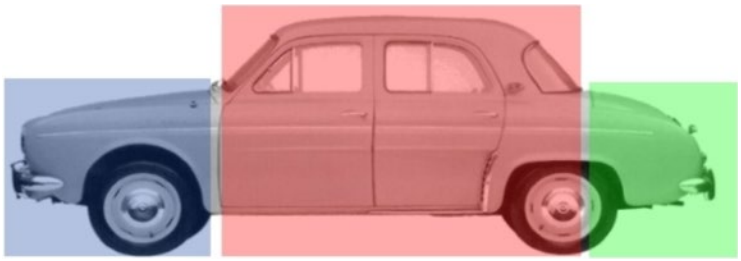

Fig. 1 *Sedan vehicle section*

A sedan car has three primary components: an engine in the front, a passenger compartment with four doors, and a luggage compartment or trunk in the back. Fig. 1 illustrates that. drag and lift were the two basic aerodynamic forces. When an automobile moves ahead, some air passes through the surface body, which resists the motion and produces drag and lift force automatically [1]. Drag is the downward force exerted by air on a car as it moves, whereas lift is the upward force exerted by air on the car. Fig. 2 illustrates the forces in play on a car.

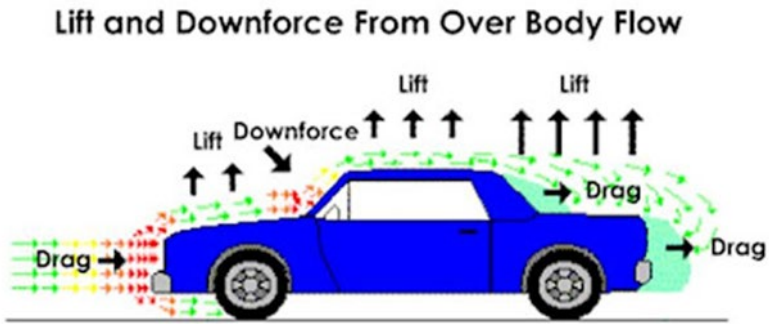

Fig. 2 *Drag and lift acting on a moving car*

Air travels in a similar manner to liquid, even though air is not as dense as liquid. When anything goes through something, it creates friction, which makes drag the most critical aerodynamic component to consider. The drag coefficient is affected by a variety of factors, including the object's general form, speed, and surface roughness. Speed and surface roughness will be constant variables in this study.

This research embarked on a journey into the realm of mathematical modelling, focusing on the application of the Polynomial Response Surface Method (PRSM) to enhance vehicle rear-end design. In some cases, the frontal area would affect the aerodynamic of a vehicle where large frontal areas such as trucks are aerodynamically inefficient [12]. In this study however, the frontal area of the sedan car was kept constant and only the rear-end of the sedan vehicle changed in parameters. The rear profile of a sedan car parameters consists of windshield angle, windshield length, trunk angle, trunk length, bumper height, trunk height and height from ground to the bumper [13].

The Polynomial Response Surface Method (PRSM) offers a systematic and efficient approach to optimize complex systems by creating surrogate mathematical models that approximate the relationships between input variables (design parameters) and output responses (performance metrics). These models enable engineers to explore design spaces, identify optimal configurations, and predict the impact of design changes without the need for exhaustive and time-consuming physical testing.

This study aimed to demonstrate how the Polynomial Response Surface Method (PRSM) can be employed as a powerful tool in vehicle rear-end design. By developing accurate surrogate models, the researchers hoped to systematically investigate the design variations, identify critical parameters, and ultimately enhance vehicle safety and performance while reducing development time and cost.

2. Methodology

2.1 Data Collection

The vehicle rear end data was collected from previous research [13] where the value of the seven parameters of the sedan vehicle, which is the wind shield length (WSL), trunk length (TL), bumper height (BH), trunk height (TH), height from ground to the bumper (BHG), wind shield angle (WSA) and trunk angle (TA) are extracted.

Int. Journal of Integrated Engineering Vol. 16 No. 8 (2024) p. 267-278

Common sedan vehicle models on the road were studied and their rear end parameters were recorded. From this data a minimum and maximum range was specified for further analysis. Table 1 and its corresponding figures illustrate the selected rear-end vehicle parameters.

Table 1 *Seven parameters of sedan vehicle and the corresponding image*

No.	Acronym	Parameter
x1	WSL	wind shield length
x2	TL	trunk length
x3	BH	bumper height
x4	TH	trunk height
x5	BHG	height from ground to the bumper
x6	WSA	wind shield angle
x7	TA	trunk angle

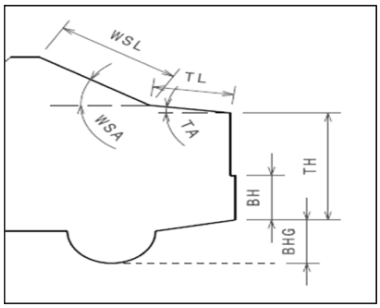

2.2 Design of Experiment (DoE)

The MATLAB R2021a software is used in this study to generate the Design of Experiment (DoE) samples. Fig. 3 shows us the CCD codes generated from Mathlab R2021a. The coded variables were then generated using the Central Composite Design (CCD), where the CCF (Central Composite Faced) sampling approach was chosen [11] as shown in Fig. 3. The actual value for the designing component was then interpreted from the coded variable. The central composite design (CCD) method was chosen as it facilitates faster design time and allows the study of the parametric interactions on the response [13]. The polynomial response surface method (PRSM) was used to generate the mathematical model and identify parametric interactions [14], [15].

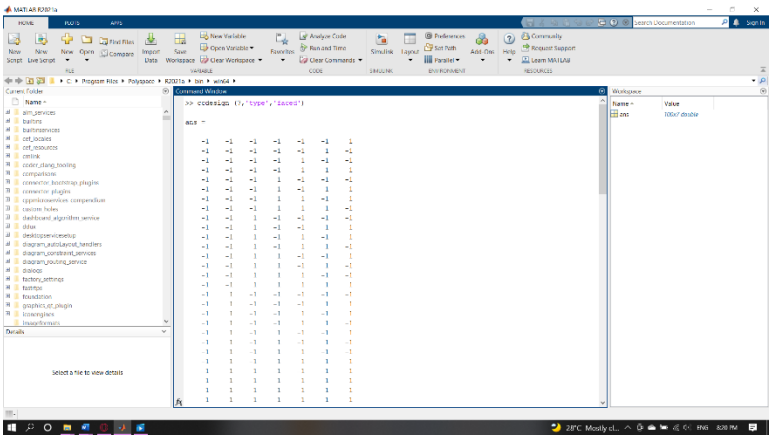

Fig. 3 *CCD codes generated from MATLAB R2021a*

The coded value of -1, 0, and 1 represents the vehicle's shortest range, median range, and maximum range. The x1 specifies the sedan car's rear wind shield length, as shown in Table 2 below. The minimum value for the x1 is 520mm, its median value is 630mm, and maximum value of 740mm. The other parameters are matched accordingly as well to the coded values generated from the DoE samples.

Table 1 *Uncoded value*

Parameter	Minimum (-1)	Median (0)	Maximum (1)
x1 (mm)	520	630	740
x2 (mm)	220	400	580
x3 (mm)	220	300	380
x4 (mm)	650	720	790
x5 (mm)	200	290	380
x6 (degree)	21°	31°	41°
x7(degree)	5°	75°	10°

2.3 Design and Drafting

The CATIA V5R21 software was used to re-design the 79 models generated from the DoE samples. Model 80 to 100 is a repetitive value of model 79 as this is done to get a good approximate of a repeated experiment. In the case of a simulation, a similar value will be generated. The vehicle models designed using CATIA V5R21 were converted to the IGES (.igs) file format to be analyzed in ANSYS 2020 R1.

The profile modelling procedure was straightforward and repeatable in terms of dimensions and length. This is the mentioned major benefit using the CCD sampling method to design many models. The vehicle design profile in the model is approximated as closely as possible to the actual size and dimensions of a sedan car to guarantee that the mistake in drag coefficient is as small as possible. The value of each coefficient of drag will be examined to select the optimal design.

2.4 Analysis and Simulation

The model of the sedan vehicle that was generated in CATIA V5R21 was then loaded into ANSYS 2020R1 for the simulation procedure. A fluid enclosure was built that acted as a fluid volume and served as the simulation's fluid domain where it was designed to simulate air flow around the vehicle. Fig. 4 displays the enclosure layout and Fig. 5 displays the enclosure set up and sizing used for this simulation.

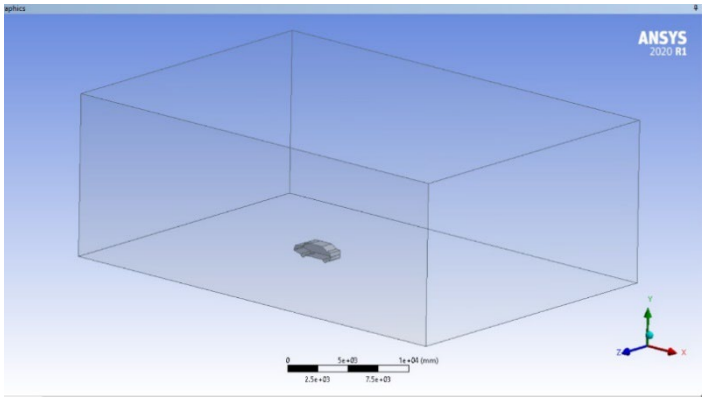

Fig. 4 *Enclosure on ANSYS 2020 R1*

The size of the enclosure was similar to previous research [13], [16]-[19] where the car was around three car lengths away from the input velocity, whereas the outlet pressure was between five and ten car lengths away from the outlet. Apart from that, the side and top walls were the same length as the intake, which was three car lengths, and a small margin of 100mm is necessary for the set up at the bottom of the car [13], [20]. The inlet, outlet, and surroundings were renamed to inlet velocity, outlet pressure, and walls for its boundary conditions.

Details View

Details of Enclosure1	
Enclosure	Enclosure1
Shape	Box
Number of Planes	0
Cushion	Non-Uniform
FD1, Cushion +X value (>0)	21600 mm
FD2, Cushion +Y value (>0)	12600 mm
FD3, Cushion +Z value (>0)	12600 mm
FD4, Cushion -X value (>0)	12600 mm
FD5, Cushion -Y value (>0)	100 mm
FD6, Cushion -Z value (>0)	12600 mm
Target Bodies	All Bodies

Fig. 5 *Enclosure setup value*

2.5 Mesh Convergence

The next step in the analysis was to perform mesh generation. The vehicle element and the area within the domain were generated using mesh generation. Since previous studies have not done any mesh convergence study, therefore it was done to ensure that the optimal mesh size was chosen. For the first element, the 2 meters' default element size was used. Then, half of the default element size is used which is 1 meter, and lastly half of 1-meter element size is used which is 0.5 meters. Fig. 6 displays the density of the elements in the meshing. The analysis for the three different element size was done and the drag coefficient (Cd) was compared between the three-

Int. Journal of Integrated Engineering Vol. 16 No. 8 (2024) p. 267-278

element size. The steady state model was selected for this analysis to compute the understeer gradient of the vehicle which in physical terms translates to the comfort of driving the vehicle over a range of lateral acceleration.

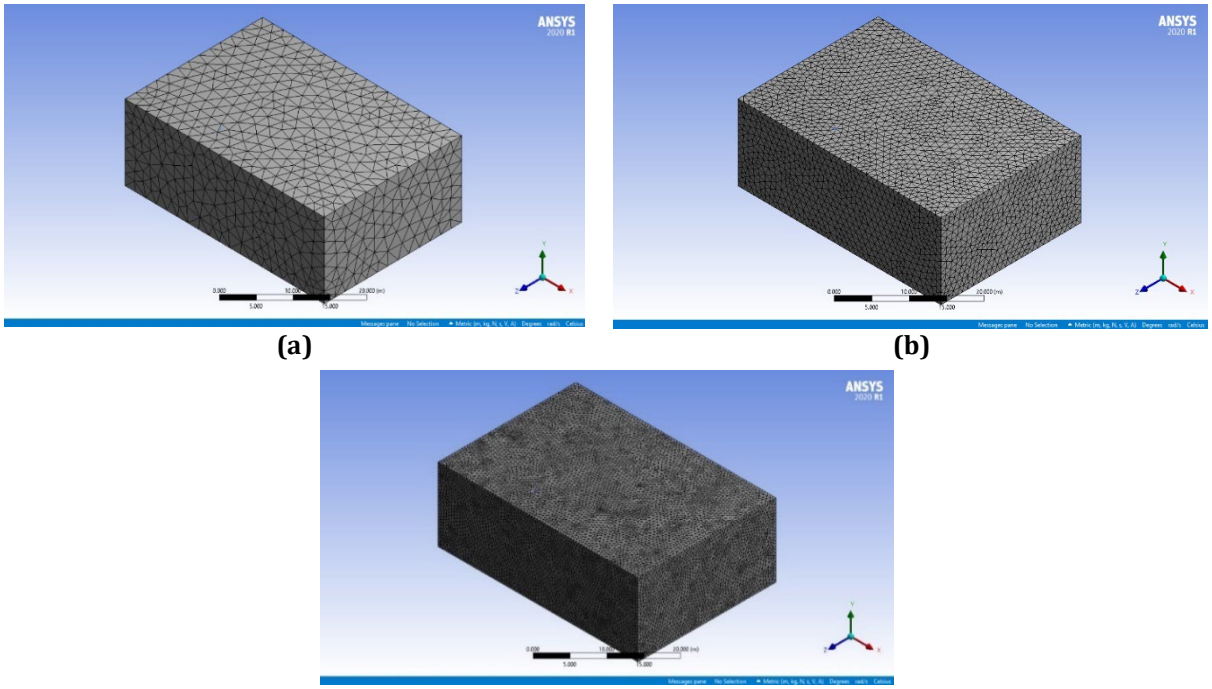

Fig. 6 *(a) 2m element size; (b) 1m element size; and (c) 0.5m element size*

3. Results and Discussion

3.1 Model Generation

The CAD model of the vehicle was generated based on the data collected. The vehicle's front specifications were kept constant to guarantee that the drag force is exclusively influenced by the rear of the vehicle. Fig. 7 and Table 3 displays the CAD data and the design parameters for model 71 which has the lowest drag coefficient among the other 79 models.

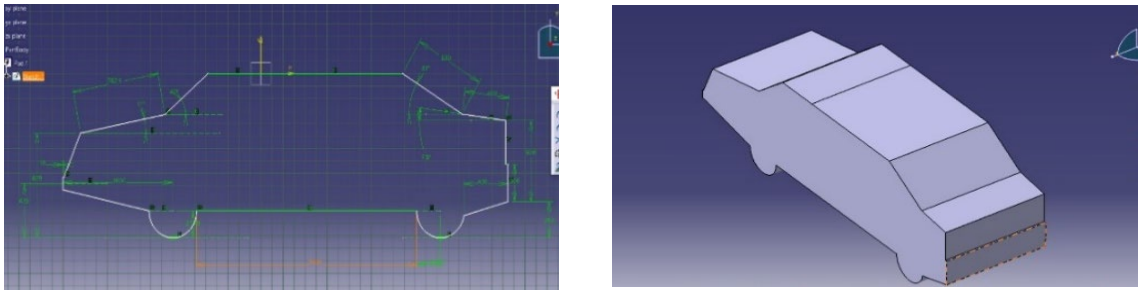

Fig. 7 *Model 71 on CATIA V5R21*

Table 3 *The parameters for model 71*

Parameters		Value
x1	WSL	630mm
x2	TL	400mm
x3	BH	300mm
x4	TH	650mm
x5	BHG	290mm
x6	WSA	31°
x7	TA	7.5°

3.2 Mesh Convergence Study

Based on the mesh convergence analysis done, the best mesh size (1 m) was chosen. Table 4 displays the results of the mesh convergence of three random models analysed, which were model 17, model 23, and model 51. When the element size was reduced to 0.5 m, all the C_d values for mode 17, model 23, and model 51 were at the lowest, at 0.43623, 0.45552, and 0.45462, respectively. When the size of elements was reduced, the time required to complete the simulation increased notably. This happened because the number of nodes and elements increased, making the mesh finer. The finer the mesh, the higher the number of nodes and elements, the higher the accuracy of the simulation and the higher time taken to complete the simulation. Based on the results obtained, the 1m element size was selected as it offered the best trade-off between the Cd accuracy and analytical computational time.

Table 4 *Mesh convergence study*

Mesh Analysis of Cd Result						
Model	17		23		51	
Cd	Time	Cd	Time	Cd	Time	
Default element size (2 m)	0.43916 (163 iterations)	39s	0.46203 (300 iterations)	64.8s	0.45644 (300 iterations)	69s
50% of number 1 element size (1 m)	0.43867 (109 iterations)	42s	0.46862 (112 iterations)	44s	0.45608 (300 iterations)	92s
50% of number 2 element size (0.5 m)	0.43623 (116 iterations)	138s	0.45552 (199 iterations)	242s	0.45462 (168 iterations)	207s
Error % between (1m) & (0.5m) element size	0.55%		2.88%		0.32%	

3.3 CATIA Design and ANSYS Simulation

The Catia and Ansys designs and data were analyzed. The best 10 rear end designs were displayed Table 5 together with the coed values and the respective actual values and equivalent drag force. Fig. 8 illustrates the rear end shapes for the 10 best models with the lowest Cd values obtained from the ANSYS simulations. The drag coefficient (Cd) range falls between 0.46 to 0.471. The models are displayed in the Cd ascending order.

Table 5 *The 10 lowest Cd value*

Model No.	Design Matrix														Drag Coefficient
	Coded Value							Actual Value							
	X1	X2	X3	X4	X5	X6	X7	X1	X2	X3	X4	X5	X6	X7	
71	0	0	0	-1	0	0	0	630	400	300	650	290	31	7.5	0.46076
19	-1	1	-1	-1	1	-1	1	520	580	220	650	380	21	10	0.46428
3	-1	-1	-1	-1	1	-1	-1	520	220	220	650	380	21	5	0.46482
43	1	-1	1	-1	1	-1	-1	740	220	380	650	380	21	5	0.46486
33	1	-1	-1	-1	-1	-1	-1	740	220	220	650	200	21	5	0.46511
51	1	1	-1	-1	1	-1	-1	740	580	220	650	380	21	5	0.46971
65	-1	0	0	0	0	0	0	520	400	300	720	290	31	7.5	0.47018
11	-1	-1	1	-1	1	-1	1	520	220	380	650	380	21	10	0.47061
17	-1	1	-1	-1	-1	-1	-1	520	580	220	650	200	21	5	0.47070
27	-1	1	1	-1	1	-1	-1	520	580	380	650	380	21	5	0.47072

Int. Journal of Integrated Engineering Vol. 16 No. 8 (2024) p. 267-278

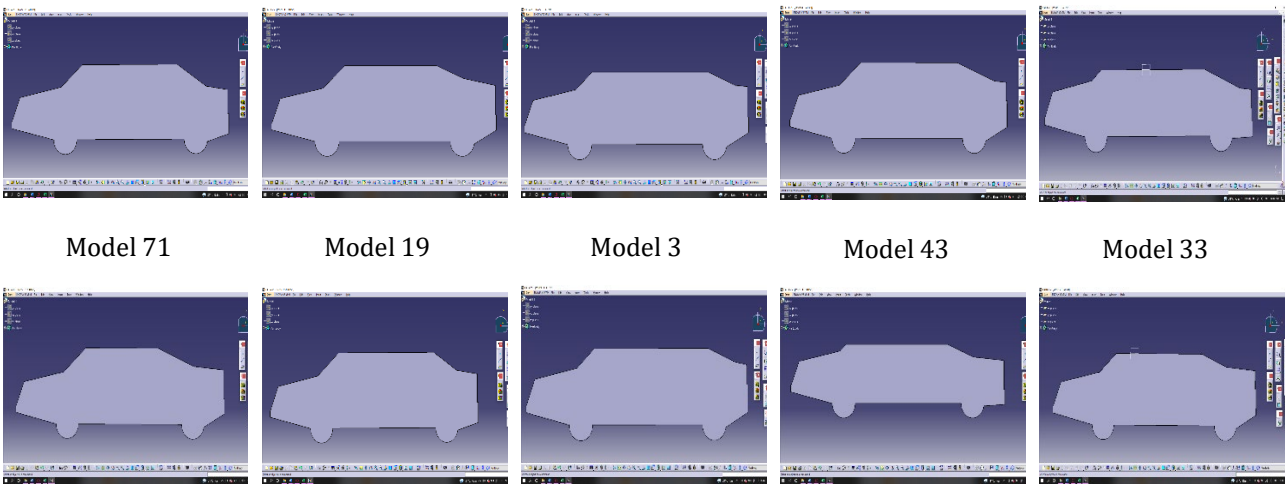

Fig. 8 *10 model for the lowest Cd value*

Model 71 has the lowest drag coefficient value of 0.46076, as can be seen in Table 5. Following that, model 19 has a drag coefficient of 0.46428, making it the second preferred model. The Cd difference between the two models was only 0.00352 or 0.0076% difference. Besides that, model 3 has been placed third, with a drag coefficient of 0.46482. Between model 19 and model 3, the difference in Cd value was 0.00054 or 0.0012%. The highest Cd value recorded was at 0.59165 in the 79 simulations run.

The intention of this study was to find out if the sedan vehicle's rear end affects the vehicle's aerodynamics considerably. The value of the drag coefficient is commonly affected by various parameters in rear-end vehicles. The following section will assess the parametric influences. Fig. 9 shows a zoomed in image of model 71 which has the lowest Cd value. It is to be noted that any rear-end add-on devices, such as a spoiler, wing, diffuser, or vertex generator, which are commonly used to minimize the coefficient of drag is not considered in this study.

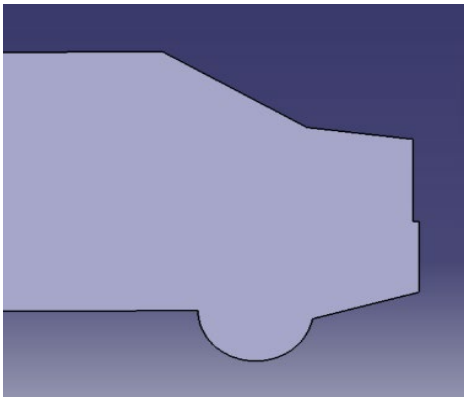

Fig. 9 *Rear end shape for Model 71*

3.4 Mathematical Modelling and Polynomial Response Surface Method (PRSM)

The Cd values that were obtained from the ANSYS simulations are tabulated to generate the mathematical model in MATLAB R2021a. The Polynomial Response Surface Method (PRSM) was used to generate the math model through the MBC Model Fitting App. Table 6 shows the summary statistics obtained. The equation yielded a R^2 value of 92.6% and an RMSE of 0.006986. This value shows that the data obtained from the analysis has minimal error and can be used to obtain the best fit graph with a high measure of goodness of fit.

The mathematical model for the Cd data is as shown in the equation below. Based on the equation, it can be observed that only parameter x1, x2, x5 and x6 have some degree of individual influence on the Cd value. The windshield angle, x6 with the constant value of 0.0042682 has the highest influence on the rear end aerodynamics. Previous research that studied the front-end parameters [21], [22] also reflected upon the front-end windshield angle as one of the prominent parameters of influence. The next prominent parameter is the height of the bumper,

x5. However, the constant values for each of these parameters are not statistically significant thus it will not be having a tangible effect on the aerodynamic influence on the rear end.

Table 6 *Summary statistics for PRSM model fitting*

Summary Statistics	
Observation	100
Parameters	19
Box-Cox	1
PRESS RMSE	8.031e-3
RMSE	**6.986e-3**
R^2	**0.926**

$$\begin{aligned} y1 = {} & 0.044523 + 0.00066838x_1 - 0.00009032x_2 - 0.0014364x_5 - 0.0042682x_6 - 0.00000068185x_1^2 \\ & + 0.00000010882x_1x_2 - 0.00000020589x_1x_3 + 0.00000019502x_1x_4 + 0.0000044134x_1x_6 \\ & + 0.0000012863x_2x_6 + 0.00000090254x_3^2 - 0.00000047949x_3x_4 - 0.00000020193x_3x_5 \\ & + 0.00000039581x_4x_5 + 0.0000021715x_4x_6 + 0.0000015485x_4x_7 + 0.000001886x_5^2 \\ & + 0.0000047343x_5x_6 \end{aligned} \quad (1)$$

The following Fig. 10 to Fig. 13 show the interaction between 2 parameters that were captured in the math model above. The advantage of the PRSM method is that it can give insights in parametric interaction from the math models generated. The surface plot shown in Fig. 10 is the product of parameter X1 and X6 which is wind shield length and wind shield angle. From the graph, when the value of X1 increases to the maximum, which is 740mm, and X6 to the maximum, 41°, the drag coefficient also increases to the maximum value.

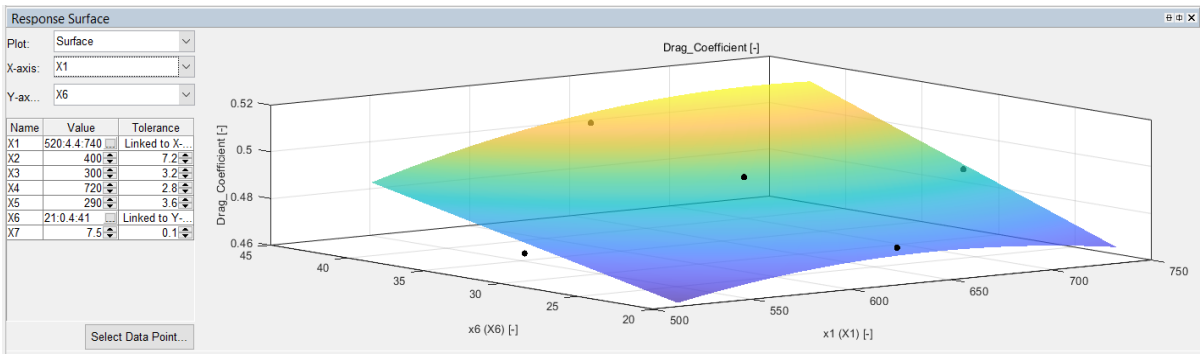

Fig. 10 *The interaction of wind shield length (x_1) and wind shield angle (x_6)*

Besides that, the interaction between X2 and X6 was also taken into consideration where X2 is the trunk length of the sedan car. The longer the trunk of the sedan vehicle, the higher the value of the drag coefficient produced at the rear end of the sedan vehicle.

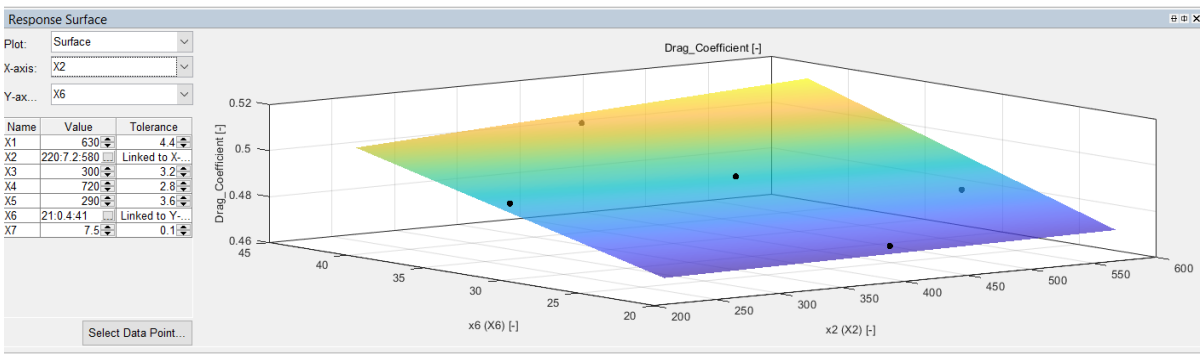

Fig. 11 *The interaction of trunk length (x_2) and wind shield angle (x_6)*

Other than the trunk length and wind shield angle, the parameters of X4 and X5 also affect the drag coefficient produced at the rear end of the sedan vehicle where the two parameters were the trunk height and the bumper

Int. Journal of Integrated Engineering Vol. 16 No. 8 (2024) p. 267-278

height from the ground. From the figures, when X4 in Fig. 12 was at its maximum value, a higher value of drag coefficient was produced.

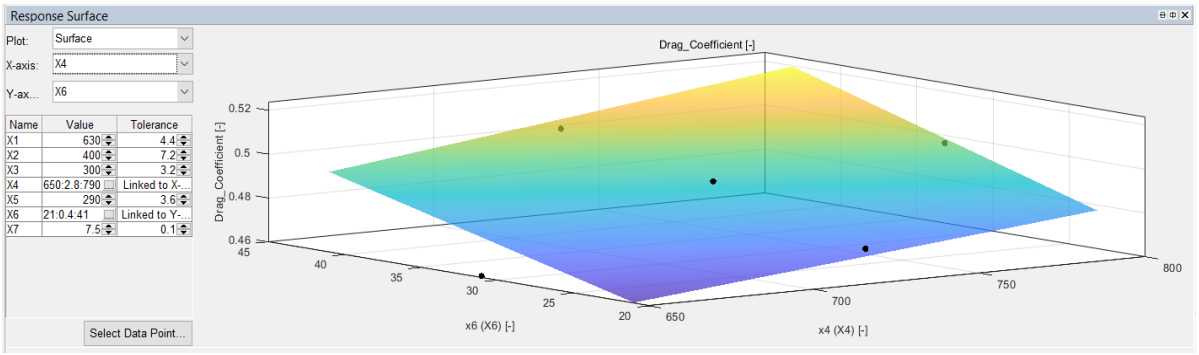

Fig. 12 *The interaction of trunk height (x_4) and wind shield angle (x_6)*

Meanwhile X5 in Fig. 13 also contributes to a high value of drag coefficient when X5 is in its maximum value.

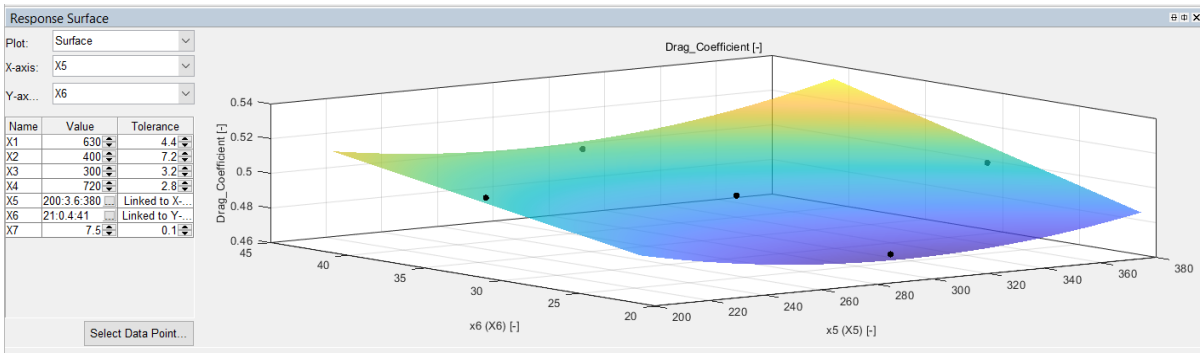

Fig. 13 *The interaction of height from ground to the bumper (x_5) and wind shield angle (x_6)*

3.5 Velocity and Pressure Contour

3.5.1 Velocity Contour

The maximum and minimum velocity contours for models 71, 19, and 3 are shown in Fig. 14. On a path line along the car, the velocity field around the car is projected and determined. To depict the airflow around the vehicle, a path line is employed. The blue colour denotes a place where velocity is at its lowest and is near to zero, whereas the turquoise and green vectors denote a region where velocity magnitude is greater.

The contact zone on the contour with the highest velocity is defined as the region where air moves at the fastest pace. The maximum velocity contour value for model 71 is 25.3372 m/s. The highest velocity for model 19 is 22.9 m/s, while the maximum velocity for model 3 is 22.6 m/s, as evidenced by the contour.

The relationship between pressure and velocity can be seen in the pressure and velocity contours for models 71, 19, and 3. The pressure and velocity are inversely proportional. The lower the pressure, the higher the velocity acting on the vehicle's surface. The contour is essential because it shows the most pressured area and the fastest-moving zone.

3.5.2 Pressure Contour

Fig. 15 displays a pressure contour that depicts the location of the highest pressure for models 71, 19, and 3. The pressure at model 71 reaches a maximum of 104.058 Pa and a low of -363.157 Pa. Next, for model 19, the maximum and minimum pressure values are 104.712 Pa and -297.173 Pa, respectively. Finally, the maximum and minimum pressure values for the third model, model 3, are 106.159 Pa and -288.240 Pa, respectively. The highest impact location is shown by the pressure contour. Even though model 71 has the lowest drag coefficient value, it also has the lowest pressure at 104.058 Pa. The next model which is model 19 has the second highest pressure acting on it which is at 104.712 Pa and finally model 3 which has the highest value of pressure acting on it which is 106.159 Pa. The greater pressure point appears on the stagnation point of the bumper on the front end for Model 71, Model 19, and Model 3.

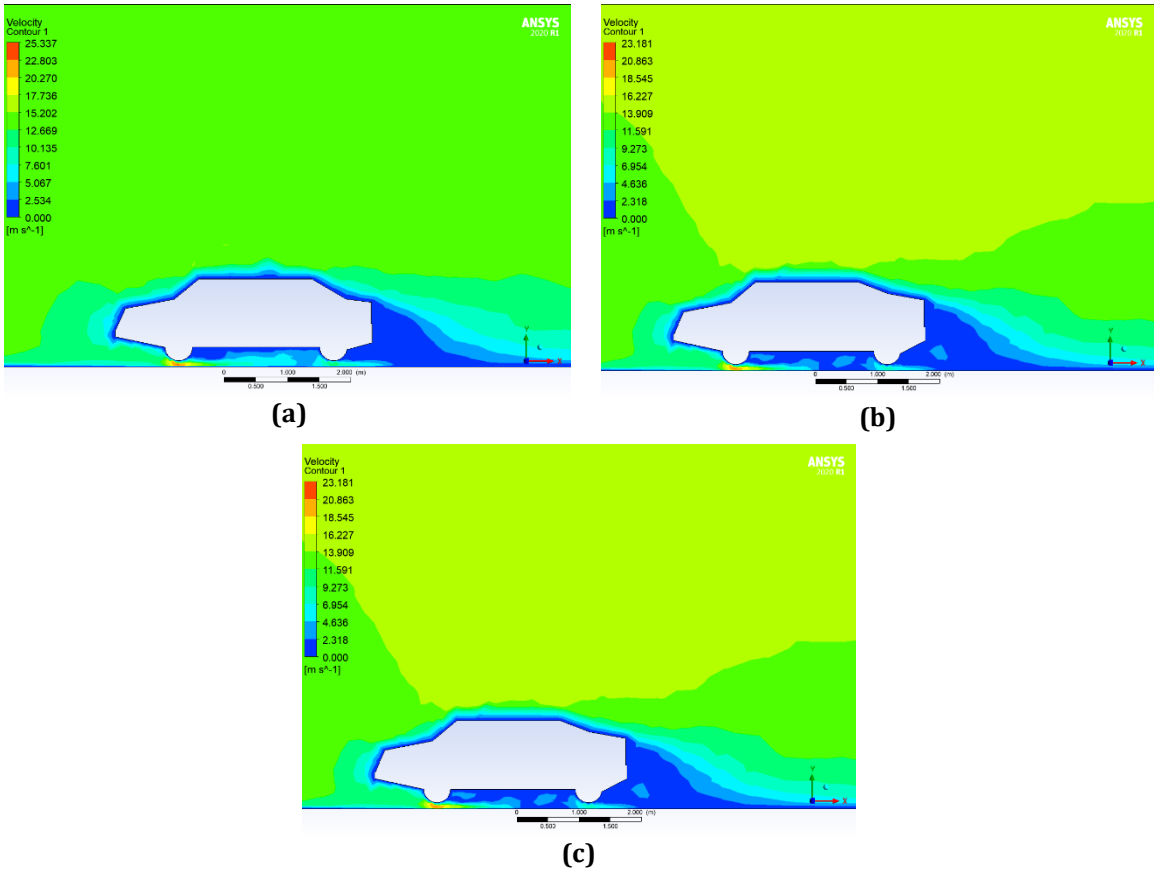

Fig. 14 *Velocity contour for (a) Model 71; (b) Model 19; and (c) Model 3*

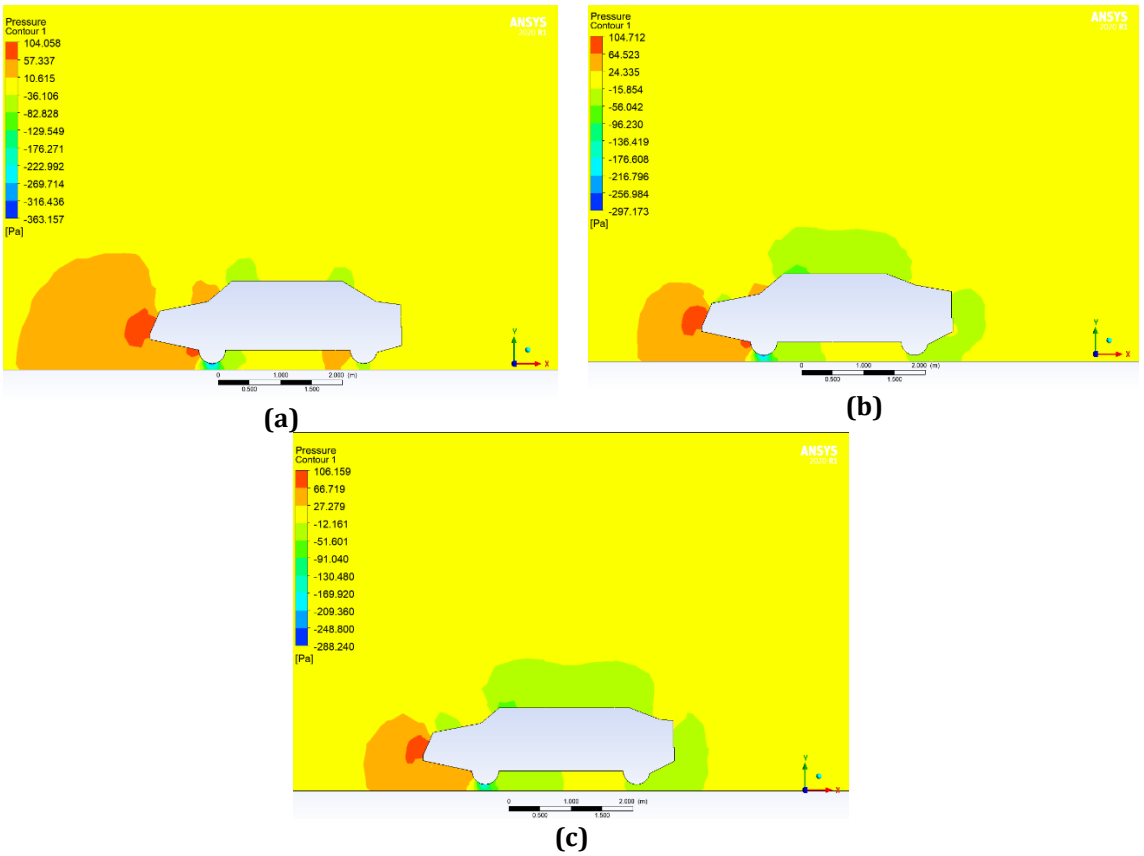

Fig. 15 *Pressure contour for (a) Model 71; (b) Model 19; and (c) Model 3*

4. Conclusion and Recommendation

The study's goal of examining the influence of the drag coefficient, Cd on the rear end of a sedan vehicle is accomplished. Although the front end of the car contacted the air initially, it was observed that there is still a drag effect at the back of the car. The analysis was conducted using the Ansys Fluent programme, which focused solely on the vehicle's external geometry. The maximum and minimum coefficients of drag observed were 0.59165 and 0.46076, respectively. From the MATLAB R2021a, through the Polynomial Response Surface Method (PRSM), the parameter X6, which is the wind shield angle plays an important role in changing the value of drag coefficient of the sedan vehicle. The higher the angle of the wind shield, the higher the drag coefficient will be. In conclusion, the rear end vehicle parameters do not seem to largely contribute to the aerodynamic stability of the model. The effect is very minimal though present.

The car's design does influence the drag effect of the vehicle. The design studied is primarily rectangular in shape without any rounded curves. Future research may focus on the influence of a curving rear end to determine the drag coefficient values.

Acknowledgement

This research was not funded by any grant. The authors would like to thanks to Universiti Teknologi MARA.

Conflict of Interest

Authors declare that there is no conflict of interest regarding the publication of the paper.

Author Contribution

The authors confirm contribution to the paper as follows: ***study conception and design:*** *Kausalyah Venkatason, Walferd Cornell;* ***data collection:*** *Walferd Cornell;* ***analysis and interpretation of results:*** *Kausalyah Venkatason, Walferd Cornell, Shasthri Sivaguru;* ***draft manuscript preparation:*** *Kausalyah Venkatason, Walferd Cornell, Shasthri Sivaguru. All authors reviewed the results and approved the final version of the manuscript.*

References

[1] Hetawal S., Gophane M., Ajay B. K., & Mukkamala Y. (2014). Aerodynamic study of formula SAE car. Procedia Engineering, 97, 1198–1207. https://doi.org/10.1016/j.proeng.2014.12.398

[2] Vinayagam, P., Rajadurai, M., Balakrishnan, K., & Priya, G. M. (2017). Design modification on Indian road vehicles to reduce aerodynamic drag. International Journal of Advanced Engineering, Management and Science, 3, 850–854. https://doi.org/10.24001/ijaems.3.8.6

[3] Mohamed-Kassim, Z., & Filippone, A. (2010). Fuel savings on a heavy vehicle via aerodynamic drag reduction, Transportation Research Part D: Transport and Environment, 15, 275–284. https://doi.org/10.1016/j.trd.2010.02.010

[4] Carmeli, M. S., Castelli-Dezza, F., Galmarini, G., Mastinu, G., & Mauri, M. (2014). A urban vehicle with very low fuel consumption: Realization, analysis and optimization. 2014 Ninth International Conference on Ecological Vehicles and Renewable Energies (EVER), Monte-Carlo, Monaco. https://doi.org/10.1109/EVER.2014.6844113

[5] Levin, J., & Rigdal, R. (2011). Aerodynamic analysis of drag reduction devices for SAAB 9-3 by CFD. Master's Thesis, Chalmers University of Technology.

[6] Jory, K., & Satheesh, A. (2013). Computational drag analysis in the under-body for a sedan type car model. 2013 International Conference on Energy Efficient Technologies for Sustainability, Nagercoil, India. https://doi.org/10.1109/ICEETS.2013.6533481

[7] Kang, S. O., Jun, S.O., Park, H. I., Song, K. S., Kee, J. D., Kim, K. H. &Lee, D. H. (2012). Actively translating a rear diffuser device for the aerodynamic drag reduction of a passenger car. International Journal of Automotive Technology, 13, 583–592. https://doi.org/10.1007/ s12239-012-0056-x

[8] Senthilkumar, P. B., Parthasarathy, M., Aravind, L., Narayanan, R. G. S., Vegesh, B., & Sam Nelson, D. R. (2022). Design and analysis of a rear diffuser in a sedan car. Materials Today: Proceedings, 59, 1324–1339. https://doi.org/10.1016/j.matpr.2021.11.542

[9] Sivaraj, G., Parammasivam, K. M., Prasath, M. S., Vadivelu, P., & Lakshmanan, D. (2021). Flow analysis of rear end body shape of the vehicle for better aerodynamic performance. Materials Today: Proceedings, 47, 2175–2181. https://doi.org/10.1016/j.matpr.2021.05.521

[10] Nizam Sudin, M., Azman Abdullah, M., Anuar Shamsuddin, S., Redza Ramli, F., & Mohd Tahir, M. (2014). Review of research on vehicles aerodynamic drag reduction methods. International Journal of Mechanical & Mechatronics Engineering 14, 35-47.

[11] Kausalyah, V., Shasthri, S., Abdullah, K. A., Idres, M. M., Shah, Q. H., & Wong, S. V. (2015). Vehicle profile optimization using central composite design for pedestrian injury mitigation. Applied Mathematics & Information Sciences,9, 197-204. http://dx.doi.org/10.12785/amis/090125
[12] Ramya, P., Kumar, A. H., Moturi, J., & Ramanaiah, N. (2015). Analysis of flow over passenger cars using computational fluid dynamics. International Journal of Engineering Trends and Technology, 29, 170–176. https://doi.org/10.14445/22315381/IJETT-V29P232
[13] Kausalyah, V., Shafiq, M. S., & Shasthri, S. (2020). Analysis of the influence of the rear end sedan vehicle profile on the aerodynamic efficiency. ARPN Journal of Engineering and Applied Sciences, 15, 8245.
[14] Chalageri, G. R., Billur, S., Shreeshail, M. L., Raju, G. U., & Kottursheṭtar, B. B. (2022). Design optimization of light motor vehicle rear twist axle. AIP Conference Proceedings, 2421, 020002. https://doi.org/10.1063/5.0079095
[15] Stabile, P., Ballo, F., Gobbi, M., & Previati, G. (2023). Multi-objective structural optimization of vehicle wheels: A method for preliminary design. Optimization and Engineering, https://doi.org/10.1007/s11081-023-09833-9
[16] Loya, A., Iqbal, A., Nasir, M. T., Ali, H., Khan, M. Z. U., & Imran, M. (2019). Automotive aerodynamics analysis using two commonly used commercial software. Engineering, 11, 22–32. https://doi.org/10.4236/eng.2019.111003
[17] Ansari, A. R. (2017). CFD Analysis of aerodynamic design of Tata Indica car. International Journal of Mechanical Engineering and Technology, 8, 344-355.
[18] Darko, D., Drazan, K., Zeljko, I. & Mato, K. (2010). Car design as a new conceptual solution and CFD analysis in purpose of improving aerodynamics. FISITA World Automotive Congress 2010, Budapest, Hungary. https://go.fisita.com/store/papers/FISITA2010/FISITA2010-SC-P-11
[19] Liu, T., Chen, Z., Zhou, X., & Zhang, J. (2018). A CFD analysis of the aerodynamics of a high-speed train passing through a windbreak transition under crosswind. Engineering Applications of Computational Fluid Mechanics, 12, 137–151. https://doi.org/10.1080/19942060.2017.1360211
[20] Ye, H., Hu, P., & Lu, S. (2009). Numerical analysis of the effect of ground clearance on a simplified car model. 2009 International Conference on Mechatronics and Automation, Changchun, China. https://doi.org/10.1109/ICMA.2009.5246707
[21] Kausalyah, V., Shasthri, S., Abdullah, K. A., Idres, M. M., Shah, Q. H., & Wong, S. V. (2014). Optimisation of vehicle front-end geometry for adult and pediatric pedestrian protection. International Journal of Crashworthiness, 19, 153–160. https://doi.org/10.1080/13588265.2013.879506
[22] Gilhaus, A. M., & Renn, V. E. (1986). Drag and driving-stability-related aerodynamic forces and their interdependence - Results of measurements on 3/8-scale basic car shapes. SAE Technical Paper, 860211. https://doi.org/10.4271/860211